JOURNAL OF AIRCRAFT
Vol. 37, No. 3, May–June 2000

Far-Field Pressure Estimation of a Plate from the Interpolated Acceleration Distribution

Daniel Blacodon*
ONERA, 92322 Châtillon Cedex, France
Dominique Brenot†
Commissairat à l'Energie Atomique, 91191 Gif sur Yvette, France
and
Alain Julienne‡
ONERA, 92322 Châtillon Cedex, France

Prediction methods of noise radiated by vibrating structures are of great interest in many applications. Normal acceleration measurements at the radiator surface can be used in combination with a method based on the Rayleigh integral to deduce the far-field radiation corresponding to the excitation sources. This method is very attractive because it is based mainly on the wave-number spectra computed by two-dimensional discrete Fourier transform. The acceleration distribution data are collected with an array of transducers in most practical cases. The spatial sampling period follows the Nyquist theorem up to time frequency F_{MAX}. The acoustic computation from measured data is inaccurate up to F_{MAX} for some observation directions because of the limited domain in which the wave-number spectra are available. A solution is proposed in this paper to remove this limitation. The wave-number spectra computational domain is extended by interpolating the acceleration distribution. This technique is applied in estimation of the far-field pressure radiated by a steel-baffled plate tested in an anechoic chamber. Comparisons between experimental measurements and estimated amplitudes carried out with interpolated data are in good agreement in all spatial directions up to F_{MAX}.

Nomenclature

C_L	= phase speed in a steel, 5000 m/s
c	= reference speed of sound, 340 m/s
f	= frequency
$f_{m,n}$	= natural frequency of the mode m, n
h	= plate thickness
k	= $2\pi f/c$, acoustic wave number
k_x	= longitudinal structural wave number
$k_{x\,\max}$	= $\pi/\Delta x$
k_y	= transverse structural wave number
$k_{y\,\max}$	= $\pi/\Delta y$
L_x, L_y	= plate dimensions
m, n	= modes
N_x, N_y	= measurement array accelerometer numbers
$\tilde{p}(r, \theta, \varphi, f)$	= far-field pressure sound at point (r, θ, φ) and at frequency f
(r, θ, φ)	= spherical coordinates
t	= time
(x, y, z)	= Cartesian coordinates
β_x, β_y	= trace of the acoustic wave number on the plate ($\beta_x = k \sin\theta\cos\varphi$, $\beta_y = k \sin\theta \sin\varphi$)
$\Gamma(k_x, k_y, f)$	= two-dimensional spatial Fourier transform of $\tilde{\gamma}(x, y, f)$ with respect to x and y
$\gamma(x, y, t)$	= acceleration distribution
$\tilde{\gamma}(x, y, f)$	= Fourier transform of $\gamma(x, y, t)$ with respect to t
Δx	= L_x/N_x sampling interval on the x axis
Δy	= L_y/N_y sampling interval on the y axis
δ	= delta function
ξ	= damping factor
ρ_s	= mean density of steel
ρ_0	= mean density of air

Presented as Paper 98-2217 at the AIAA/CEAS 4th Aeroacoustics Conference, Toulouse, France, 2–4 June 1998; received 27 July 1998; revision received 25 October 1999; accepted for publication 29 October 1999.

*Research Engineer, DSNA/PARA, BP 72-29 avenue de la Division Leclerc; blacodon@onera.fr. Member AIAA.
†Departmental Manager, Centre de Saclay, DPE; brenot@vandoise.cea.fr.
‡Unit Manager, DSNA/BREC, BP 72-29 avenue de la Division Leclerc; julienne@onera.fr.

Introduction

FAR-FIELD prediction methods are of great interest in many current applications. They are used, for example, to evaluate the sound radiated by vibrating structures from near-field measurements performed with an array of microphones[1,2] or with a synthetic antenna.[3] Other arrangements based on the acceleration distribution of the structure can be used to estimate the far-field sound. One of these techniques, using the Rayleigh integral,[4] is applied to the data from an experiment performed in an anechoic chamber. The structure studied is a steel plate mounted in a baffle. This simple case is examined because many structures of practical interest, such as walls and floors of a building and factory machinery casings or vehicle parts, can be modeled with sufficient accuracy by rectangular flat plates.

The plate studied was equipped with a matrix of accelerometers. The size of the elementary mesh of this array was defined to generate the acceleration distribution measurement over the plate surface according to the Nyquist theorem up to a frequency F_{MAX}. A two-dimensional discrete Fourier transform is performed on the data collected by the array to obtain the wave-number spectra required for the acoustic computation.

The difficulty is essentially caused by the problem of replicated sources corresponding to the spectral aliasing phenomenon caused by sampling in the spatial frequency domain. This is inevitably encountered when the spatial frequency spectrum is not bandlimited. This problem weakly corrupts the far-field computation up to F_{MAX}. Then, another more penalizing drawback arises in this study. For our observation directions the acoustic calculation has to be performed with wave-number components larger than those provided by the discrete Fourier transform. So, the far-field pressure cannot be accurate up to F_{MAX} because of those periodically replicated wave number.

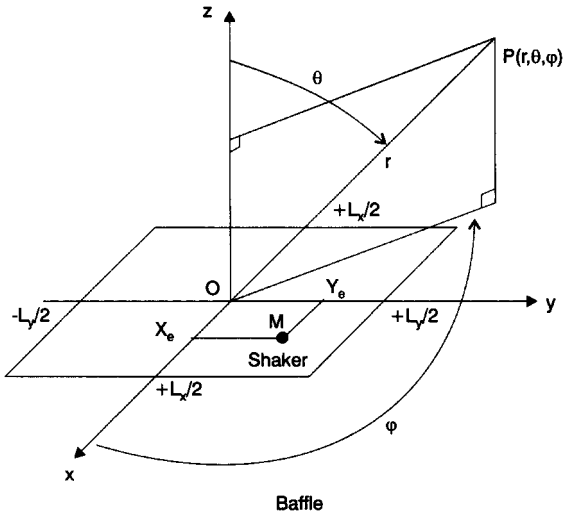

Fig. 1 Geometry of the far-field pressure estimation of a plate inserted in a baffle from acceleration distribution measurements.

The objective of the paper is to propose a way to reduce the aliasing error by displacing the periodically replicated sources farther away from the actual ones by interpolating the measurements. This approach is illustrated by comparing experimental measurements and far-field estimations with and without data interpolation.

Acoustic Field Pressure Radiated by Baffled Plate

Consider the geometry of the problem sketched in Fig. 1. A rectangular plate is simply supported on edge on a rigid baffle located in the plane $z = 0$. This plate is mechanically excited at a single point $M(x_e, y_e)$ and radiates an acoustic wave field in the semispace $z > 0$. The extrapolation problem consists in determining the far-field pressure from the acceleration distribution $\gamma(x, y, t)$ at an observation point $p(r, \theta, \varphi)$ and at any arbitrary frequency f.

This problem can be solved by the Rayleigh integral:

$$\tilde{P}(r, \theta, \varphi, f) = \frac{\rho_0 e^{ikr}}{2\pi r} \int_{-L_x/2}^{L_x/2} \int_{-L_y/2}^{L_y/2} \exp[-ik(x \sin\theta\cos\varphi + y \sin\theta \sin\varphi)]\tilde{\gamma}(x, y, f)\, dx\, dy \quad (1)$$

This result is expressed in terms of the two-dimensional Fourier transform of the acceleration distribution $\tilde{\gamma}(x, y, f)$:

$$\Gamma(\beta_x, \beta_y, f) = \int_{-L_x/2}^{L_x/2} \int_{-L_y/2}^{L_y/2} \exp[-i(x\beta_x + y\beta_y)]\tilde{\gamma}(x, y, f)\, dx\, dy \quad (2)$$

where $\beta_x = k \sin\theta\cos\varphi$ and $\beta_y = k \sin\theta \sin\varphi$. Substituting the preceding expression into Eq. (1), the pressure field can be written in the following form:

$$\tilde{P}(r, \theta, \varphi, f) = \frac{\rho_0 e^{ikr}}{2\pi r} \Gamma(\beta_x, \beta_y, f) \quad (3)$$

We are not interested in the phase relationship in the far field, but rather in the sound intensity pressure level

$$|\tilde{P}(r, \theta, \varphi, f)|^2 = (\rho_0/2\pi r)^2 |\Gamma(\beta_x, \beta_y, f)|^2 \quad (4)$$

This is the formula used in acoustic computations.

Spatial Sampling and Far-Field Sound Prediction Maximum Frequency

The limitations in using Eq. (4) are introduced by spatial sampling. These acoustic calculations are examined in this section.

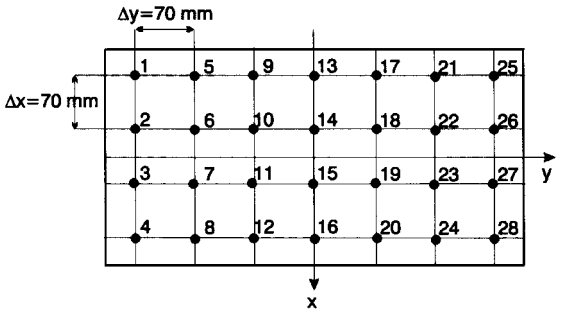

Fig. 2 Geometry of accelerometer array on the plate surface.

Limitation Caused by the Spatial Sampling of the Plate

The assumption is made that the measurement array comprises $N = N_x \cdot N_y$ ($N_x = 4$ and $N_y = 7$) accelerometers at positions x_{n_x}, y_{n_y} located on a rectangular grid, as illustrated in Fig. 2:

$$x_{n_x} = -L_x/2 + \Delta_x\left(n_x + \tfrac{1}{2}\right), \qquad n_x = 0, 1, \ldots, N_x - 1 \quad (L_x = 0.28\ \text{m})$$

$$y_{n_y} = -L_y/2 + \Delta_y\left(n_y + \tfrac{1}{2}\right), \qquad n_y = 0, 1, \ldots, N_y - 1 \quad (L_y = 0.49\ \text{m}) \quad (5)$$

where $\Delta x = L_x/N_x = 0.07$ m and $\Delta y = L_y/N_y = 0.07$ m.

Let $\tilde{\gamma}_d(x, y, f)$ designate the time Fourier transform of the acceleration sampled by the planar array

$$\tilde{\gamma}_d(x, y, f) = \sum_{n_x=0}^{N_x-1} \sum_{n_y=0}^{N_y-1} \delta\left(x - x_{n_x}, y - y_{n_y}\right)\tilde{\gamma}(x, y, f) \quad (6)$$

The modulus squared of the two-dimensional Fourier of $\tilde{\gamma}_d(x, y, f)$ with respect to x and y is

$$|\Gamma_d(k_x, k_y, f)|^2 = \sum_{n_1}^{\infty} \sum_{n_2}^{\infty} |\Gamma_d(k_x + n_1 2k_{x\max}, k_y + n_2 2k_{y\max}, f)|^2 \quad (7)$$

where $k_{x\max} = \pi/\Delta x = 44.87$ rd/m and $k_{y\max} = \pi/\Delta y = 44.87$ rd/m.

$\Gamma_d(k_x, k_y, f)$ is doubly periodic in (k_x, k_y), with period $(2k_{x\max}, 2k_{y\max})$. Moreover there will be no replicated wave number in $|\Gamma_d(k_x, k_y, f)|^2$ if

$$|\Gamma_d(k_x, k_y, f)|^2 = 0 \quad \text{for} \quad \begin{cases} |k_x| < k_{x\max} = 44.88\ \text{rd/m} \\ |k_y| < k_{y\max} = 44.88\ \text{rd/m} \end{cases} \quad (8)$$

We shall soon establish that conditions (8) remain true up to frequency F_{MAX}.

Let us now consider a rectangular panel simply supported on an infinite rigid baffle. Its acceleration distribution induced by a monochromatic force at frequency f and at position $M(x_e, y_e)$ is [5]

$$\tilde{\gamma}(x, y, f) = \frac{f^2}{\pi\rho_s h} \times \frac{\sum_{m=1}^{\infty}\sum_{n=1}^{\infty} \sin\left[m\pi\left(x/L_x + \tfrac{1}{2}\right)\right]\sin\left[n\pi\left(y/L_y + \tfrac{1}{2}\right)\right]}{f_{mn}^2 - 2i\xi f f_{mn} - f^2} E_{mn} \quad (9)$$

where

$$E_{mn} = E_0 \sin\left[m\pi\left(x_e/L_x + \tfrac{1}{2}\right)\right] \sin\left[n\pi\left(y_e/L_y + \tfrac{1}{2}\right)\right]$$

and E_0 is the force amplitude.

Each term of this double sum indicates that $\tilde{\gamma}(x, y, f)$ has a significant value arround the resonance frequencies f_{mn}, which is

Table 1 Theoretical and experimental natural frequencies f_{mn} associated with the modes m, n

			Experimental natural frequencies	
m	n	Theoretical natural frequencies, Hz	Shaker at $x = y = 0$	Shaker at $x = -6$ cm, $y = -14$ cm
1	1	460	450	450
1	2	800	——	800
1	3	1367	1300	1300
2	1	1501	——	1600
2	2	1841	——	1800
1	4	2160	——	2100
2	3	2408	——	2300
1	5	3180	2850	3000
2	4	3201	——	——
3	1	3237	3350	——
3	2	3577	——	——
3	3	4143	——	3850
2	5	4221	——	4200
1	6	4426	——	——
3	4	4936	——	——
2	6	5467	——	5300
4	1	5666	——	5600
1	7	5899	5850	——

assumed to be negligible outside a narrow frequency band centered on f_{mn}. Below a given frequency F_{MAX}, only modes m, n satisfying

$$f_{mn} = \left(hC_L/2\pi\sqrt{12}\right)\left(k_x^2 + k_y^2\right) < F_{\mathrm{MAX}} \tag{10}$$

where

$$k_x = m\pi/L_x, \qquad k_y = n\pi/L_y \tag{11}$$

contribute to the acceleration distribution. The list of the f_{mn} up to 5899 Hz associated with modes m, n are grouped in Table 1.

The following relations between N_x and N_y and the panel modes m and n can be then deduced comparing Eqs. (8) and (11):

$$|m| < N_x, \qquad |n| < N_y \tag{12}$$

We conclude then that $\gamma(x, y, t)$ is not undersampled up to $F_{\mathrm{MAX}} = f_{m=2,n=6} = 5467$ Hz obtained from Table 1 and Eq. (12). Hereafter, the assumption will be made that the mode $m = 4$, $n = 1$ is weakly replicated in the frequency band $[0, F_{\mathrm{MAX}}]$, and thus $\gamma(x, y, t)$ will be considered as a bandlimited function in wave number until F_{MAX}.

Limitation Caused by the Far-Field Computation

Let us return to the problem of sound radiation by the baffled plate. From Eq. (7) there is no aliasing phenomenon nor periodically replicated wave number in $|\Gamma_d(\beta_x, \beta_y, f)|^2$ if $|\beta_x|$ and $|\beta_y|$ verify

$$|\beta_x| < k_{x\,\max} = 44.88 \text{ rd/m}, \qquad |\beta_y| < k_{y\,\max} = 44.88 \text{ rd/m} \tag{13}$$

We will show that the acoustic computation requires wave numbers $|\beta_x|$ and $|\beta_y|$ to be larger than $k_{x\,\max}, k_{y\,\max}$, respectively, in the experiment described in the last section. To prove this, let us replace β_x and β_y in Eq. (13) by their expressions [Eq. (2)] to obtain

$$|(2\pi f_x/c)\sin\theta\cos\varphi| < \pi/\Delta x, \qquad |(2\pi f_y/c)\sin\theta\sin\varphi| < \pi/\Delta y \tag{14}$$

We deduce from the preceding that the computation of $|\Gamma_d(\beta_x, \beta_y, f)|^2$ is correct up to

$$f_{\max} = \min(f_x, f_y) \tag{15}$$

where

$$f_x = c/2\Delta x|\sin\theta\cos\varphi|, \qquad f_y = c/2\Delta y|\sin\theta\sin\varphi| \tag{16}$$

Relations (16) also show that the frequency $f_{\max}$ depends on both the spherical angles θ, φ and the sampling periods Δx and Δy. The lowest limit $f_{\max} = 2428$ Hz is obtained for $|\sin\theta\cos\varphi| = |\sin\theta\sin\varphi| = 1$, when the observation point is on the normal to the plate, and the largest one is $f_{\max} = F_{\mathrm{MAX}}(F_{\mathrm{MAX}} = 5467$ Hz) because of the spatial sampling. Thus, $f_{\max}$ can be equal to the upper limit F_{MAX} for specific angles θ or φ, but it is generally smaller. Now consider the ideal case where $\min(f_x) = \min(f_y) = F_{\mathrm{MAX}}$ to determine the highest wave number β_x, β_y required by the acoustic computation. Inserting these two frequencies in Eqs. (14), we get

$$|\beta_x|_{\max} = |\beta_y|_{\max} = 101 \text{ rd/m} \tag{17}$$

Clearly, this result is irrelevant with Eqs. (13) because $|\beta_x|_{\max}$ and $|\beta_y|_{\max}$ are much larger than 44.88 rd/m. The components $|k_x|, k_y| > 44.88$ rd/m of $|\Gamma_d(k_x, k_y, f)|^2$ are thus periodically replicated in the wave-number domain [Eq. (7)]. This is why the acoustic computation Eq. (4) cannot be accurate up to F_{MAX} for particular observation directions.

Extension of Wave-Number Spectra Calculation

The problem just explained can be solved simply by analyzing Eqs. (16), which suggest that the size Δx and Δy of the elementary mesh of the array must be divided by three to displace the periodically replicated wave number beyond this domain:

$$0 < |\beta_x| < k_{X\,\mathrm{MAX}}, \qquad k_{X\,\mathrm{MAX}} = \pi/(\Delta x/3) = 3k_{x\,\max}$$
$$0 < |\beta_y| < k_{Y\,\mathrm{MAX}}, \qquad k_{Y\,\mathrm{MAX}} = \pi/(\Delta y/3) = 3k_{y\,\max} \tag{18}$$

representing the computational region of $|\Gamma_d(k_x, k_y, f)|^2$ for the acoustic calculation. This can be achieved using a two-dimensional interpolation method because the acceleration distribution $\tilde{\gamma}_d(x, y, f)$ has been assumed to be bandlimited in wave number until F_{MAX} [see after Eq. (12)]. The interpolated data $\tilde{\gamma}_i(x_p, y_q, f)$ in $x_p = p\Delta x/3$ and $y_q = q\Delta y/3$ are obtained from the original sequence $\tilde{\gamma}_d(x, y, f)$ using the following expression[6]:

$$\tilde{\gamma}_i(x_p, y_q, f) = \sum_{n_x}^{N_x}\sum_{n_y}^{N_y} \tilde{\gamma}_d\left(x_{n_x}, y_{n_y}, f\right) \times \frac{\sin(x_p k_{X\,\mathrm{MAX}} - n_x\pi)}{x_p k_{X\,\mathrm{MAX}} - n_x\pi} \frac{\sin(y_q k_{Y\,\mathrm{MAX}} - n_y\pi)}{y_q k_{Y\,\mathrm{MAX}} - n_y\pi} \tag{19}$$

A finite number of terms are used in the preceding expansion inducing a truncation error[7]

$$e_{N_x,N_y} \le \sqrt{\frac{\pi}{k_{X\,\mathrm{MAX}}}\frac{\pi}{k_{Y\,\mathrm{MAX}}}\sum_{p>N_x}\sum_{q>N_y}\left|\tilde{\gamma}\left(p\frac{\pi}{k_{X\,\mathrm{MAX}}}, q\frac{\pi}{k_{Y\,\mathrm{MAX}}}, f\right)\right|^2} \tag{20}$$

This error remains acceptable, as shown in the next section by comparing the far-field prediction computed from accelerometers data with and without interpolation.

Tests in an Anechoic Chamber

A simple experiment was conducted in an anechoic chamber to validate the method proposed in this paper. The experimental setup is shown in Fig. 3.

We used a steel plate of thickness $h = 12$ cm, width $L_x = 8$ cm, and length $L_y = 49$ cm. It was inserted in a baffle made of plates of expanded polystyrene covered by wooden panels with reflecting skin.

In the experiment the plate was mechanically excited at a single point by a shaker vibrating in the frequency range [0, 10 kHz] to obtain the broadband plate response. First, the shaker was centered at $x = y = 0$ in order to excite only the odd natural modes. Then it was moved to $x = -6$ cm, $y = -14$ cm to excite both odd and even natural modes.

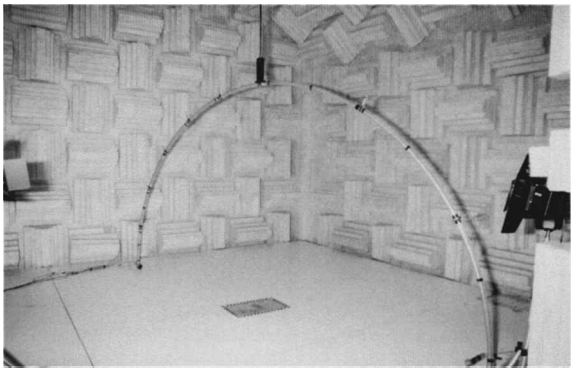

Fig. 3 Experimental setup.

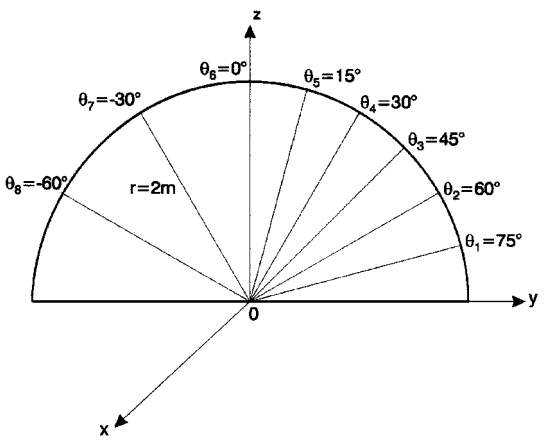

Fig. 4 Microphones location on the semicircular support.

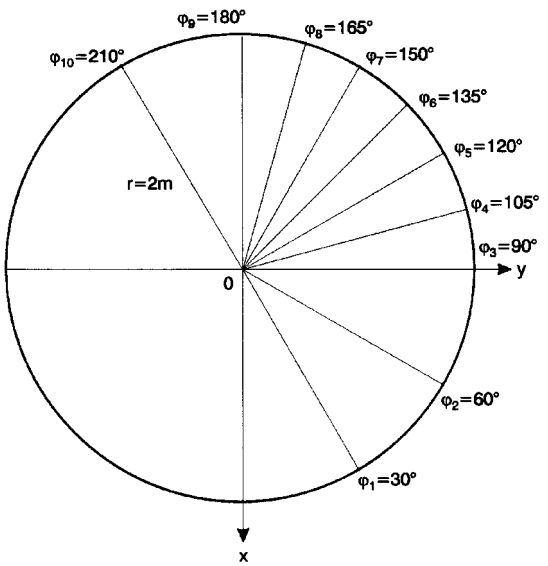

Fig. 5 Location of the semicircular support during the experiment.

The acceleration distribution was measured by four rows of seven Bruel and Kjaer 4374 accelerometers. The acoustic far-field radiated by the plate was measured by eight Aksud 4133 microphones placed on a semicircular support of radius $r = 2$ m, at angles $\theta_1 = 75$ deg, $\theta_2 = 60$ deg, $\theta_3 = 45$ deg, $\theta_4 = 30$ deg, $\theta_5 = 15$ deg, $\theta_6 = 0$ deg, $\theta_7 = -30$ deg, $\theta_8 = -60$ deg (Fig. 4). This support was moved around its main axis at 10 angles $\varphi_1 = 30$ deg, $\varphi_2 = 60$ deg, $\varphi_3 = 90$ deg, $\varphi_4 = 105$ deg, $\varphi_5 = 120$ deg, $\varphi_6 = 135$ deg, $\varphi_7 = 150$ deg, $\varphi_8 = 165$ deg, $\varphi_9 = 180$ deg, $\varphi_{10} = 210$ deg (Fig. 5), allowing the data to be collected on a semisphere sampled at 71 points.

Experimental Results

We first present the power spectral density measured by one accelerometer when the plate excitation is centered and then moved off center in order to examine the plate frequency response for these two configurations. Then the wave-number spectra corresponding to the case where the shaker is centered are displayed in order to 1) first verify the hypothesis that $|\Gamma_d(k_x, k_y, f)|^2$ is a bandlimited function with respect to k_x, k_y and 2) then illustrate the preceding discussion on the aliasing problem and its solution as achieved by interpolating the acceleration distribution. Lastly, comparisons are made between measured and predicted far-field sound pressure levels.

Plate Frequency Response

Figure 6 shows the power spectrum of accelerometer 6 (Fig. 2) when the shaker is centered. Many peaks appear corresponding to the natural frequencies of the plate. The first peaks at frequencies $f = 450$, 1250, 2850, and 3350 Hz are caused by the odd natural modes $(m = 1, n = 1)$, $(m = 1, n = 3)$, $(m = 1, n = 5)$, and $(m = 3, n = 1)$ respectively, (see Table 1). As expected, the even modes are weakly excited.

Figure 7 presents the power spectrum of the same accelerometer when the shaker is not centered. The power spectrum decreases beyond 5 kHz because of the antialiasing filter. The number of peaks is much higher than before because the odd and even natural modes are both excited. Table 1 indicates that the first frequencies ($f = 800$, 1800, and 2100 Hz) correspond to the modes $(m = 1, n = 2)$, $(m = 2, n = 2)$, and $(m = 1, n = 4)$.

Wave-Number Spectra

The plot of the acceleration wave-number spectrum $|\Gamma_d(k_x, f)|^2$ in the frequency range [0, 10 kHz] (Fig. 8) is obtained from data from the fourth column of accelerometers (i.e., accelerometers 13, 14, 15, and 16), showing that the plate is excited mainly at odd resonant frequencies because of the centered excitation (see Table 1). The

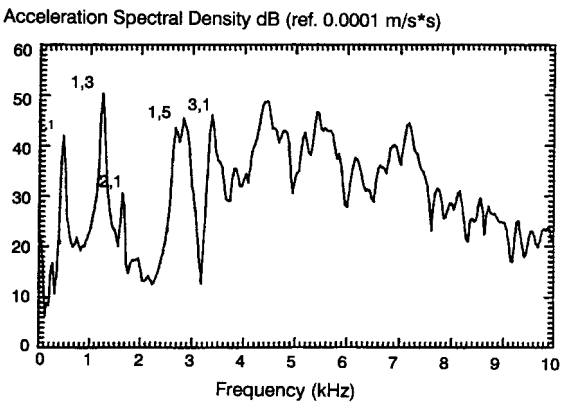

Fig. 6 Frequency spectrum of acceleration measured by accelerometer 6 in Fig. 2 when the shaker is centered on the plate.

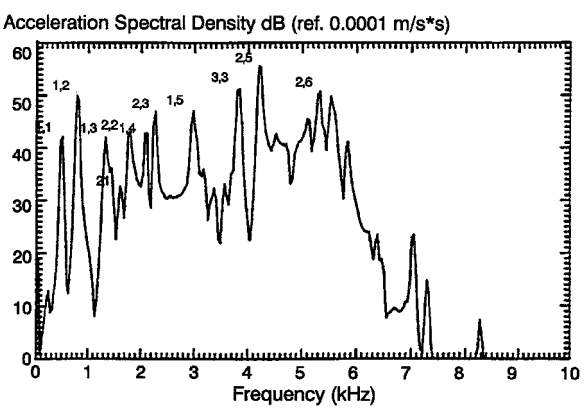

Fig. 7 Frequency spectrum measured of acceleration by accelerometer 6 in Fig. 2 when the shaker is moved off the center of the plate.

zero wave-number peak is dominant at $f = 1250$ Hz. The wave-number components are larger in the high frequency range. But, as expected, the aliasing phenomenon with respect to k_x, k_y is negligible. It corresponds to the grating lobes at the largest wave-number spectra components beyond 4.3 kHz.

The plot (Fig. 9) obtained from data collected by the third row of accelerometers (i.e., accelerometers 3, 7, 11, 15, 19, 23, and 27) also shows that the plate is excited mainly at the odd resonant frequencies. A dominant peak appears at $k_y = 11.21$ rd/m and $f = 4.2$ kHz.

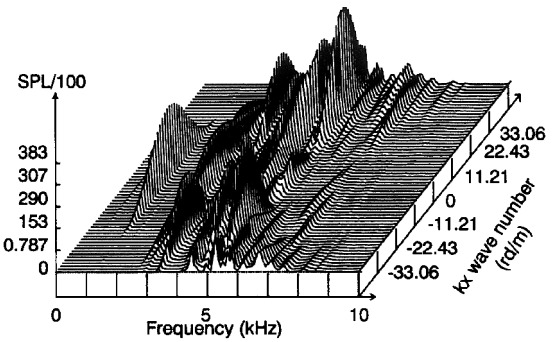

Fig. 8 k_x wave-number frequency response of the plate subjected to a centered excitation.

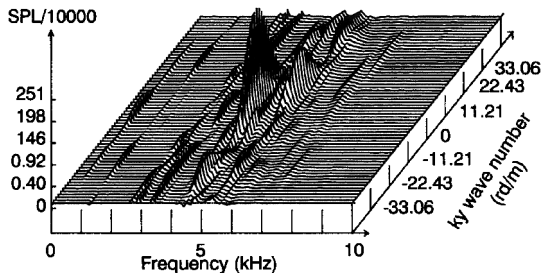

Fig. 9 k_x wave-number frequency response of the plate subjected to a centered excitation.

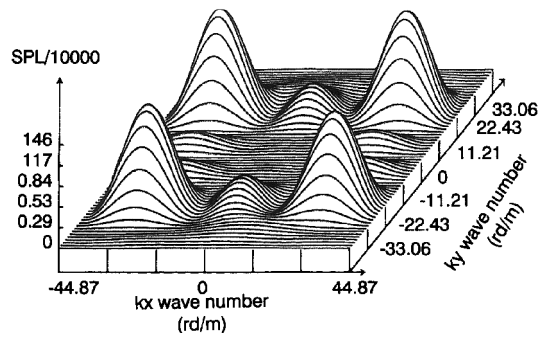

Fig. 10 Wave-number spectra computed at f = 4134 Hz from rough data in the wave-number region $(|k_x|, |k_y|) \leq$ 44.87 rd/m.

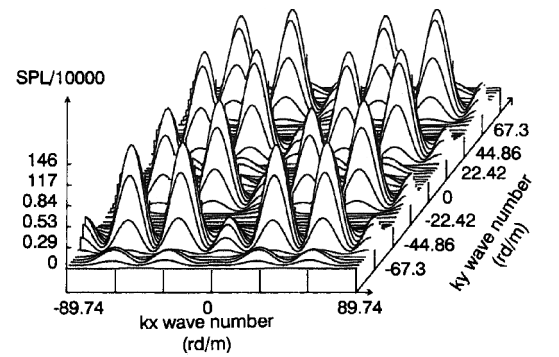

Fig. 11 Same legend as in Fig. 10, but the computation is performed in the wave-number region $(|k_x|, |k_y|) \leq$ 89.74 rd/m.

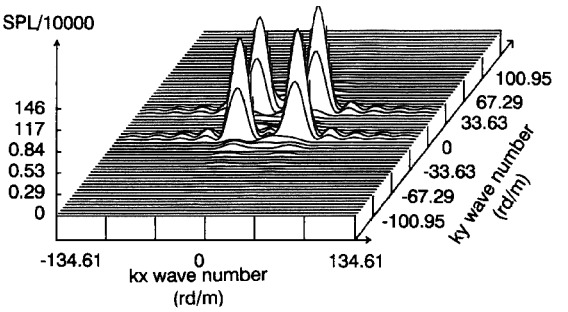

Fig. 12 Same as Fig. 11, but the computation is performed in the domain $(|k_x||k_y|) \leq$ 134.61 rd/m. with interpolated data.

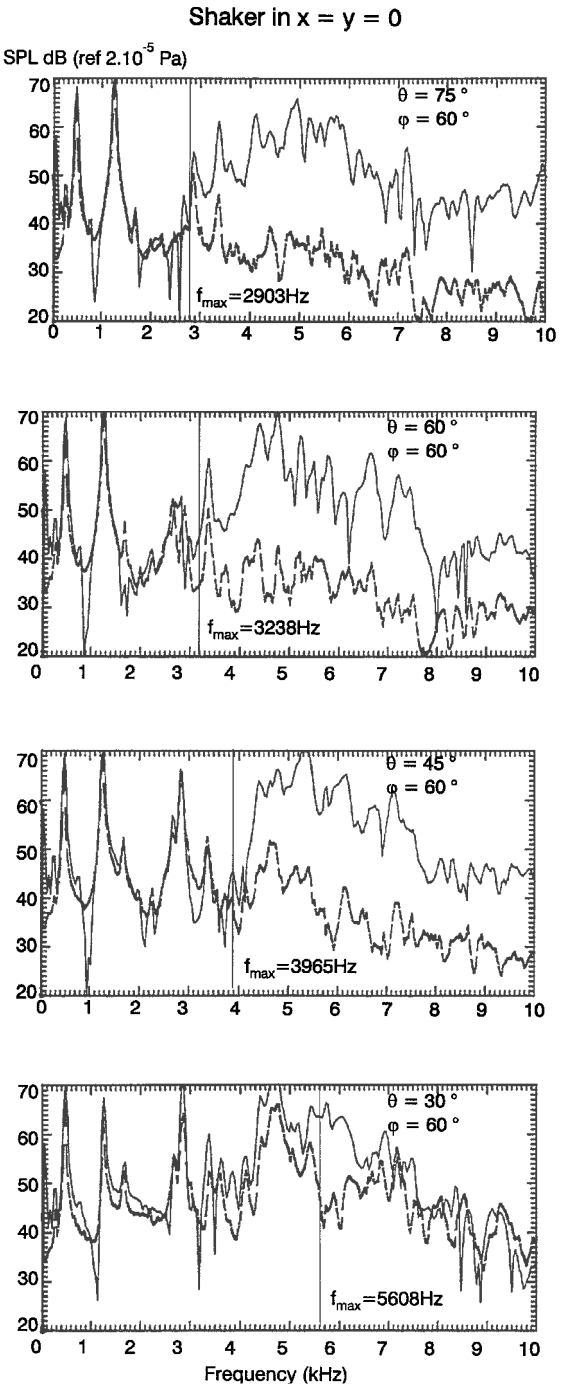

Fig. 13 Comparison between measured amplitudes (- - -) and far-field pressure predicted with initial data (——).

As before, the aliasing phenomenon with respect to k_x, k_y remains very weak.

The two-dimensional wave-number spectra computed with measured data at $f = 4.134$ KHz are presented in Fig. 10. For this frequency the actual wave-number components satisfy the conditions $(|k_x|, |k_y|) \leq 44.87$ rd/m, and this is verified because there are only four peaks centered around ($k_x = 30$ rd/m, $k_y = 22.4$ rd/m), ($k_x = 30$ rd/m, $k_x = -22.4$ rd/m), ($k_y = -30$ rd/m, $k_y = 22.4$ rd/m), and ($k_x = -30$ rd/m, $k_y = -22.4$ rd/m).

The aliasing phenomenon becomes visible in Fig. 11, which is also computed with measured data but in a larger k_x, k_y domain (i.e., $(|k_x|, |k_y|) \leq 89.74$ rd/m). The 12 peaks beyond $|k_x|, |k_y|) > 44.87$ rd/m are caused by the double periodicity introduced by the discrete Fourier transform because the plate response should be zero. The far-field sound pressure predictions estimated with these components cannot therefore be correct.

Lastly, wave-number spectra are displayed (Fig. 12) in the acoustic component region required for far-field pressure estimations (i.e., for $(|k_x|, |k_y|) \leq 101$ rd/m). The computation is carried out from data interpolated using Eq. (19). Clearly, the undesirable peaks in Fig. 11 have been displaced beyond the revelant domain in k_x, k_y. Now only the four actual peaks are left as shown in Fig. 10.

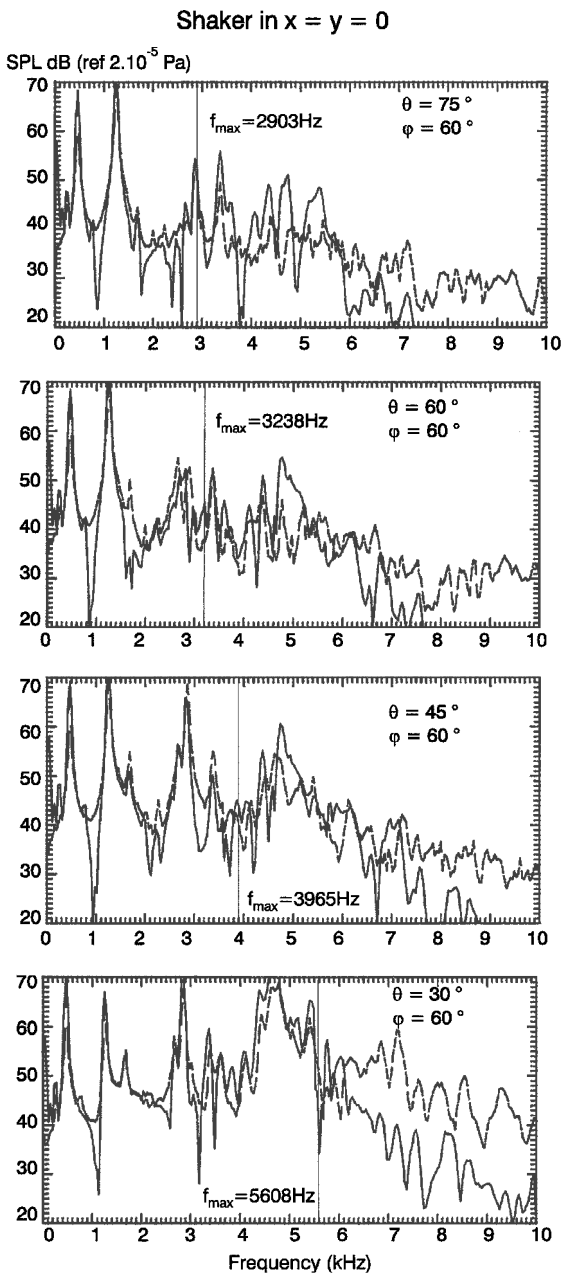

Fig. 14 Comparison between measured amplitudes (– – –) and far-field pressure predicted with interpolated data (——).

Comparison Between the Measured and Estimated Far-Field Pressure Level

The measured sound pressure field amplitudes at locations ($\theta = 75$ deg, $\varphi = 60$ deg), ($\theta = 60$ deg, $\varphi = 60$ deg), ($\theta = 45$ deg, $\varphi = 60$ deg), ($\theta = 30$ deg, $\varphi = 60$ deg) are compared with sound pressure estimates using Eq. (4) and measured accelerations. Accelerations with and without interpolation are considered.

Shaker Centered

In the first test the far-field radiated pressure is produced only by the odd natural modes of the plate.

Radiation Sound Computation Using Measured Accelerometer Data

Clearly, the agreement is very good in Fig. 13 up to a frequency close to $f_{\max}$ [computed with Eq. (15)] and depending on of the

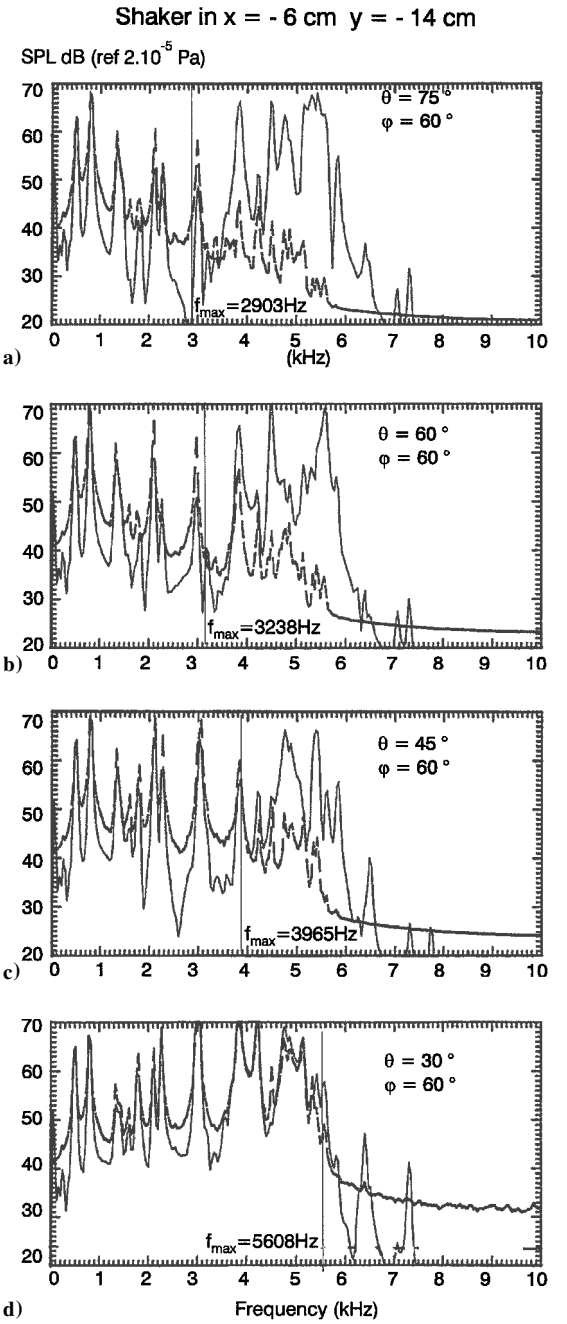

Fig. 15 Comparison between measured amplitudes (– – –) and far-field pressure predicted with initial data (——).

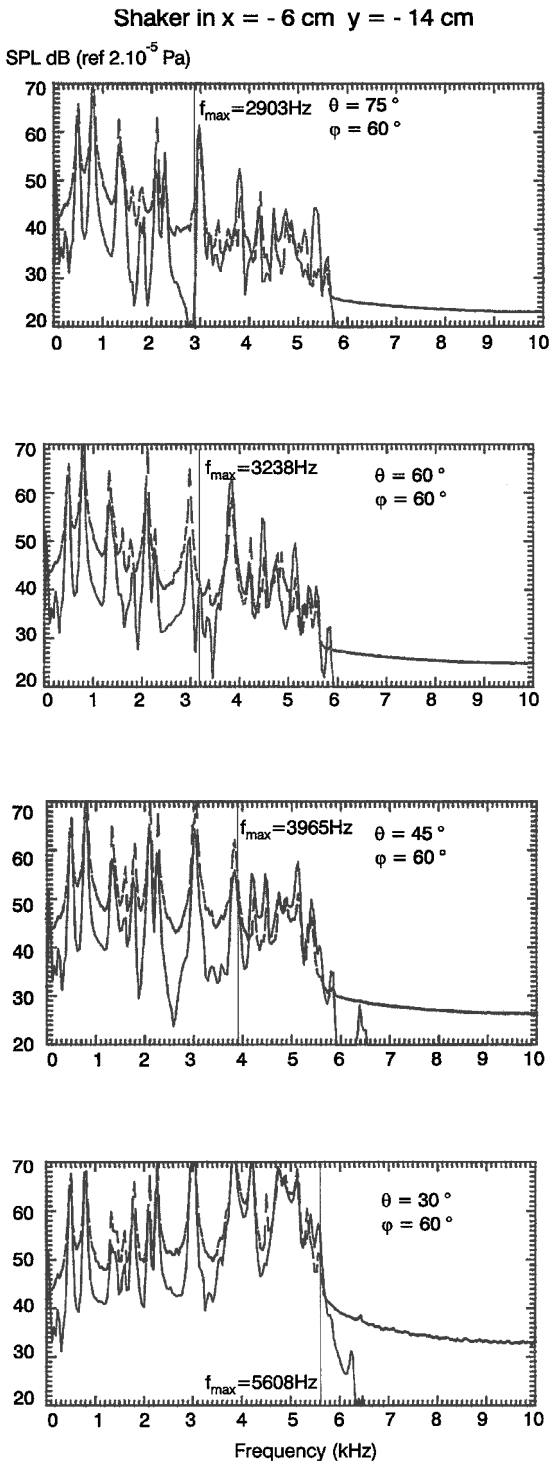

Fig. 16 Comparison between measured amplitudes (- - -) and far-field pressure predicted with interpolated data (——).

direction observations. Nevertheless, it appears that f_{max} is below F_{MAX} depending on the observation angles.

Radiation Sound Computation Using Interpolated Acceleration Data

Experimental measurements and far-field sound estimations nearly coincide beyond F_{MAX} with only slight differences on a number of peaks (Fig. 14) when the computations are carried out with interpolated data.

Shaker Noncentered

In the second test the sound radiated in the far field is produced by the odd and even natural modes of the plate. As in the preceding case, a remarkable agreement is found between the amplitude of the field measured and estimated from measured acceleration data but not up to F_{MAX} in Figs. 15a–15c and above F_{MAX} in Fig. 15d. The decrease observed in the measured amplitudes beyond 5.7 kHz is caused by an antialiasing filter. When the computations are carried out with interpolated data, measured and calculated amplitudes are again in agreement up to F_{MAX} (Fig. 16).

Conclusion

The far-field pressure radiated by a baffled steel plate subject to a point excitation was predicted using the wave-number spectra of the acceleration distribution measured by an array of accelerometers. The accelerometer array samples the acceleration distribution in accordance with the Nyquist theorem up to the frequency F_{MAX}. Nevertheless, the acoustic calculation from measured acceleration data is not accurate up to F_{MAX} anywhere in the space above the plate, because it is carried out with periodically replicated components in wave-number spectra. An interpolation method is proposed to extend the computational domain wave number, allowing the acoustic calculation up to F_{MAX} at any far-field point. This conclusion is confirmed by numerous comparisons between experimental measurements and estimated sound pressure levels.

Acknowledgment

This work was supported by DGA/DRET, French Ministry of Defense.

References

[1]Candel, S. M., and Chassaignon, C., "Radial Extrapolation of Wave Fields by Spectral Methods," *Journal of Acoustical Society of America*, Vol. 76, No. 6, 1984, pp. 1823–1828.

[2]Elias, G., and Payen, F., "Far-Field Extrapolation of Near-Field Measurement Using Inverse Method," AIAA Paper 89-1115, April 1989.

[3]Blacodon, D., Candel, S., and Elias, G., "Radial Extrapolation of Wave Fields from Synthetic Measurements of the Nearfield," *Journal of Acoustical Society of America*, Vol. 82, No. 3, 1987, pp. 1060–1072.

[4]Junger, M. C., *Sound Structure and Their Interaction*, Massachusetts Inst. of Technology Press, Cambridge, MA, 1972, pp. 88, 89.

[5]Lesueur, C., "Rayonnement Acoustique des Structures Vibroacoustiques, Interactions Fluide-Structure," *Collection de la Direction des Etudes et Recherches d'Electricité de France*, Edition Eyrolles, Paris, 1988.

[6]Schaffer, W., and Rabiner, R., "A Digital Signal Processing Approach to Interpolation," *Proceedings of the IEEE*, Vol. 61, No. 6, 1973, pp. 692–702.

[7]Papoulis, A., "Error Analysis in Sampling Theory," *Proceedings of the IEEE*, Vol. 54, No. 7, 1966, pp. 947–955.